





ORIGINAL ARTICLE

MicroRNA-143/Musashi-2/KRAS cascade contributes positively to carcinogenesis in human bladder cancer

Takuya Tsujino^{1,2}  | Nobuhiko Sugito¹ | Kohei Taniguchi³  | Ryo Honda¹ | Kazumasa Komura^{2,3}  | Yuki Yoshikawa² | Tomoaki Takai² | Koichiro Minami² | Yuki Kuranaga¹ | Haruka Shinohara¹  | Yoshihisa Tokumaru⁴ | Kazuki Heishima¹ | Teruo Inamoto² | Haruhito Azuma² | Yukihiro Akao¹

¹United Graduate School of Drug Discovery and Medical Information Sciences, Gifu University, Gifu, Japan

²Department of Urology, Osaka Medical College, Osaka, Japan

³Translational Research Program, Osaka Medical College, Osaka, Japan

⁴Department of Surgical Oncology, Graduate School of Medicine, Gifu University, Gifu, Japan

Correspondence

Yukihiro Akao, United Graduate School of Drug Discovery and Medical Information Sciences, Gifu University, Gifu, Japan.
Email: yakao@gifu-u.ac.jp

Funding information

Japan Agency for Medical Research and Development, Grant/Award Number: 16cm0106202 h0001

Abstract

It has been well established that microRNA (miR)-143 is downregulated in human bladder cancer (BC). Recent precision medicine has shown that mutations in BC are frequently observed in *FGFR3*, *RAS* and *PIK3CA* genes, all of which correlate with RAS signaling networks. We have previously shown that miR-143 suppresses cell growth by inhibiting RAS signaling networks in several cancers including BC. In the present study, we showed that synthetic miR-143 negatively regulated the RNA-binding protein Musashi-2 (MSI2) in BC cell lines. MSI2 is an RNA-binding protein that regulates the stability of certain mRNAs and their translation by binding to the target sequences of the mRNAs. Of note, the present study clarified that MSI2 positively regulated KRAS expression through directly binding to the target sequence of KRAS mRNA and promoting its translation, thus contributing to the maintenance of KRAS expression. Thus, miR-143 silenced KRAS and MSI2, which further downregulated KRAS expression through perturbation of the MSI2/KRAS cascade.

KEYWORDS

bladder cancer, KRAS, miR-143, Musashi-2, RNA-binding protein

1 | INTRODUCTION

Bladder cancer (BC) is the most common malignancy of the urinary tract. According to the American Cancer Society, approximately 79 000 new cases of BC and over 18 000 deaths were estimated to have occurred in the USA alone in 2017.¹ Recent precision medicine showed that gene alternations in BC were frequently observed in *FGFR3*, *RAS* and *PIK3CA*,^{2,3} all of which are correlated with RAS signaling networks. Among these networks, that of KRAS, in particular, is extremely complicated. Moreover, KRAS regulates more than 10 effector signaling pathways, and its expression is promoted mainly

by receptor tyrosine kinases (RTK), including *FGFR3*.^{4,5} Previous studies reported on the networks of KRAS.^{6,7} In addition, microRNAs (miR) that directly target KRAS signaling impede KRAS-driven tumorigenesis.⁷ Previous studies including ours demonstrated that miR-143 suppresses KRAS-mediated tumorigenesis.⁸⁻¹⁰ Moreover, miR-143 is strongly downregulated in several cancers,^{9,11-14} including BC,^{15,16} and it inhibits cell proliferation by suppressing both signaling pathways of PI3K/AKT and MAPK, which are downstream of KRAS effector signaling pathways, as well as KRAS in BC.¹⁷

The Musashi gene is a consequence of earlier gene duplication, and humans have two related genes, Musashi-1 (*MSI1*) and

Musashi-2 (*MSI2*). *MSI1* and *MSI2* share approximately 75% amino acid identity in their overall structure and belong to a family of RNA-binding proteins.¹⁸ *MSI2* post-transcriptionally regulates mRNA processing by binding to the recognition motifs located at the 3'UTR of target mRNAs, similar to *MSI1*. *MSI2* preferentially interacts with an ACCUUUUUAGAA motif and other poly-U sequences,¹⁹ UAG motifs, and UAG-containing motifs ± additional flanking nucleotides.^{20,21} The Musashi proteins were first linked to cancer based on studies showing elevated expression of *MSI1* in gliomas,²² medulloblastomas,²³ and hepatomas.²⁴ *MSI2* was identified as part of a translocation event with *HoxA9* in chronic myeloid leukemias that preserved *MSI2* RNA-binding motifs,²⁵ also implicating *MSI2* in cancer development. The past several years have been marked by a surge of reports elucidating the frequency and mechanisms of involvement of *MSI2*, in particular, in multiple forms of human cancer,^{19,26-28} including BC.²⁹ Like *MSI1*, moreover, Dong et al³⁰ reported that *MSI2* is directly regulated in a negative way by miR-143.

In the present study, we clarified the correlation between *KRAS* and *MSI2*, both of which are targets of miR-143. Notably, knockdown of *MSI2* induced downregulation of *KRAS*, and overexpression of *MSI2* upregulated *KRAS* without causing an increase in the level of *KRAS* mRNA. These results indicated that *MSI2* post-transcriptionally regulated *KRAS* expression. Furthermore, by using a luciferase reporter assay and surface plasmon resonance (SPR), we demonstrated that *MSI2* positively regulated *KRAS* expression through directly binding to the target sequence UAGUA in the 3'UTR region of *KRAS* mRNA. Taken together, our findings indicated the extremely potent anticancer activity of synthetic miR-143 (syn-miR-143), and it enabled us to clarify and better understand the role of the novel miR-143/*MSI2*/*KRAS* cascade in human BC.

2 | MATERIALS AND METHODS

2.1 | RNA immunoprecipitation

RNA immunoprecipitation (RIP) was carried out with a RIP-assay Kit (Medical & Biological Laboratories Co., Ltd., Aichi, Japan) according to the manufacturer's instructions.

2.2 | RNA-stability measurements

The RNA polymerase II transcriptional inhibitor 5,6-dichlorobenzimidazole riboside (DRB) was procured from Tokyo Chemical Industry (Tokyo, Japan). T24 cells were seeded on the day prior to transfection with the cDNA plasmid encoding *MSI2* or control vector. The cells were treated with DRB at 24 hours after transfection. Cellular RNA was harvested at time 0, 2, 4, 6 and 8 hours and used for qRT-PCR analysis of *KRAS* mRNA. RNA half-lives were calculated from linear regression of log-transformed expression values.³¹ ANCOVA was carried out on the resulting regression lines to assess statistical significance.

2.3 | Human tumor xenograft model

Animal experimental protocols were approved by the Committee for Animal Research and Welfare of Gifu University (approval no. H30-42). BALB/cSLC-nu/nu (nude) mice were obtained from Japan SLC (Shizuoka, Japan). Human bladder cancer T24 cells were inoculated into the back of each mouse. At 7 days after the inoculation, we confirmed engraftment of the tumors. When the tumor size had reached approximately 100 mm³, treatment was started. siRNA or miRNA carried by Lipofectamine RNAi MAX (Invitrogen, Carlsbad, CA, USA) was injected into the tumor every 2 days for a total of three times. Each group contained three mice. Tumor volume was calculated by the formula: $0.5236 L1 (L2)^2$, where L1 is the long axis and L2 is the short axis.

Other methods are shown in Data S1.

3 | RESULTS

3.1 | Impact of *KRAS* on proliferation of bladder cancer cell lines

To investigate the function of *KRAS* as an oncogene in human BC, we first assessed the association between cell growth and *KRAS* and that between it and *HRAS* in BC cell lines T24 and 253JB-V. Knockdown of *HRAS* by use of siRNA significantly suppressed cell proliferation, and knockdown of *KRAS* resulted in a more potent growth inhibition than that obtained with knockdown of *HRAS* (Figure 1A). In addition, *KRAS* effector signaling proteins, AKT and ERK1/2, were downregulated by both knockdowns (Figure 1B). Of note, this knockdown was more prominent in T24 cells, which have an *HRAS* mutation, not a *KRAS* one. These results suggested that *KRAS* contributed considerably to cell proliferation in BC, as did *HRAS*.

3.2 | Syn-miR-143 directly silences the key genes of *KRAS* networks and *MSI2*

Previously, we reported that miR-143 inhibited cell proliferation with apoptosis through silencing PI3K/AKT and MAPK signaling pathways, which are major growth-related effector signal pathways in *KRAS* networks in BC.^{17,32} As shown in Figure 2A, the expression levels of miR-143 were extremely downregulated in both T24 and 253JB-V cells. Recently, we developed a chemically modified miR-143 that has potent RNase-resistant anticancer activity (Figure S1). This syn-miR-143 silences not only *KRAS* but also *KRAS* effector signaling molecules, AKT and ERK.¹⁰

To clarify how *KRAS* networks contribute to carcinogenesis and cell growth in BC, we introduced syn-miR-143 into T24 cells, which induced apoptosis to a greater extent than that obtained with Ambion miR-143 (Ambion, Carlsbad, CA, USA), probably as a result of extreme silencing of *KRAS* networks (Figure S2).¹⁰ As shown in Figure 2B, ectopic expression of syn-miR-143 led to significant growth inhibition in both cell lines. Western blot analysis

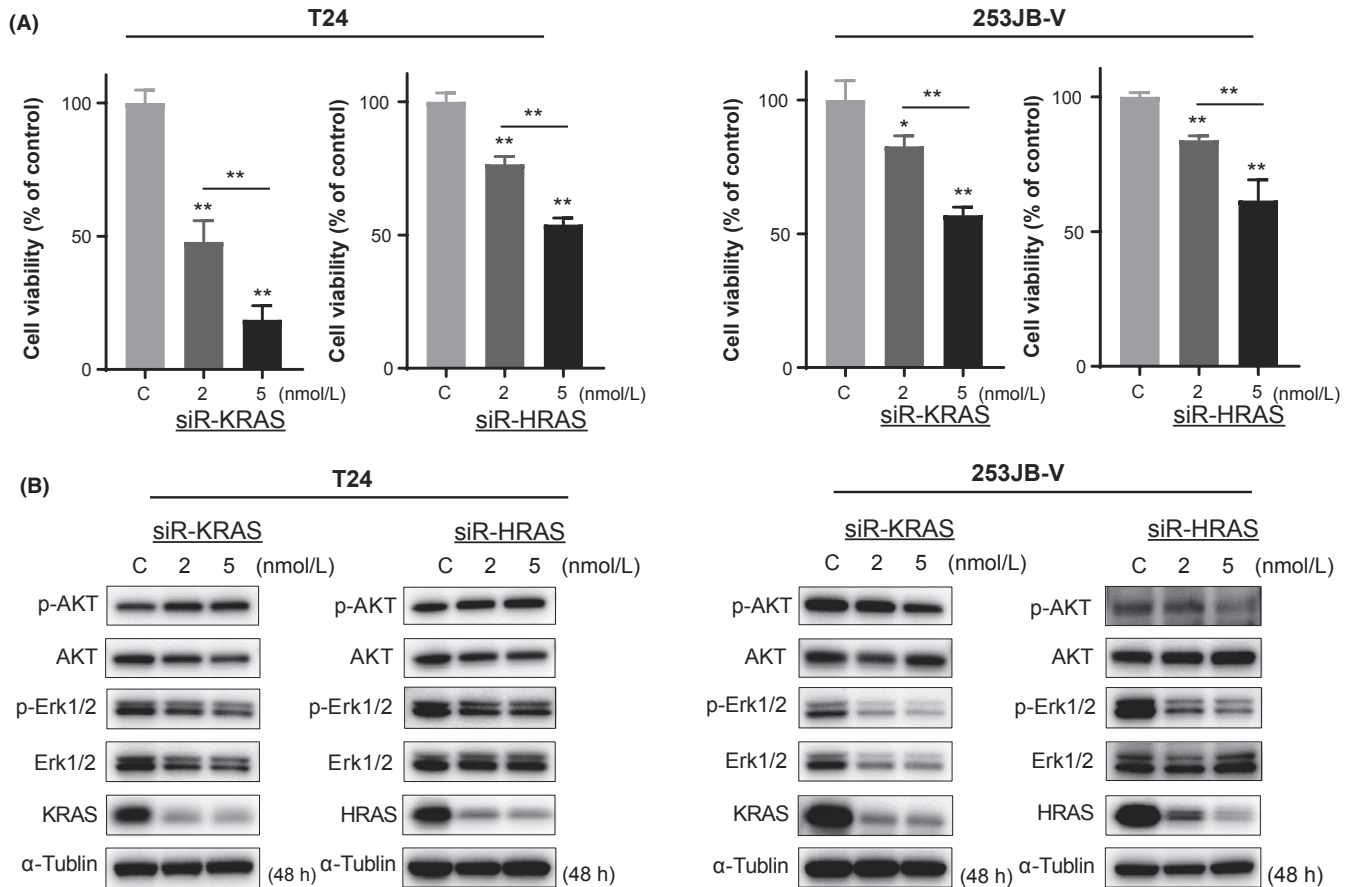


FIGURE 1 KRAS strongly contributes to cell growth in bladder cancer (BC) cell lines. Cell growth inhibition (A) and protein expression (B) with siR-KRAS or siR-HRAS in T24 and 253JB-V cells. * $P < .05$; ** $P < .01$. Means + SD indicated by error bars are shown

indicated that syn-miR-143 strongly decreased the expression of KRAS protein and its effector signaling proteins AKT and ERK1/2. Interestingly, RNA-binding protein MSI2 was also downregulated. MSI2 was recently reported as a target of miR-143 in cervical cancer³⁰ and has the fourth-most frequent genetic alterations in BC across almost all major cancers as assessed in The Cancer Genome Atlas (TCGA) BC cohort using the cBioPortal for Cancer Genomics (cBioPortal; Figure S3), and has specific target sequences recognized by miR-143 according to in silico prediction tools in TargetScan. In addition, treatment with antagomiR-143 reversed the growth inhibition and lowered protein levels of both KRAS and MSI2 elicited by syn-miR-143 (Figure 2C). To examine whether miR-143 directly bound to the 3'UTR region of MSI2 mRNA, we cloned the 3'UTR of MSI2 mRNA containing the possible miR-143 binding site in a reporter plasmid. As a result, luciferase activity of wild-type pMIR-MSI2 was inhibited after cotransfection with miR-143 and the reporter plasmid DNA in T24 cells (Figure 2D). In contrast, decrease in luciferase activity was abrogated in the case of mutated binding sites. Together, these results indicated that miR-143 could silence MSI2 expression at the translation step and inhibit BC cell proliferation, in part, through suppression of MSI2 expression. Hence, next we focused on the oncogenic function of MSI2 and the interaction between MSI2 and KRAS.

3.3 | Musashi-2 is upregulated in clinical tumor samples of BC

We examined the expression of MSI2 in 10 samples from BC patients by western blot analysis. Clinicopathological findings of the patients are shown in Table S1. As shown in Figure 3A, MSI2 was upregulated in six of the 10 clinical BC samples examined compared with its level in normal bladder tissues in the same patients, and expression of miR-143 was downregulated in all cases according to qRT-PCR results (Figure 3B). Therefore, all cases of MSI2 overexpression corresponded to downregulation of miR-143. In addition, qRT-PCR analysis of MSI2 mRNA showed upregulation in T24 and 253JB-V cells, and the increase was more prominent in T24 cells than in 253JB-V cells (Figure 3C). Based on these results, we focused on T24 cells in the following experiments.

3.4 | Relationship between MSI2 and KRAS or HRAS in T24 cells

To examine the interaction between MSI2 and KRAS, we carried out knockdown and overexpression of MSI2 by using siRNA (Figure S4) and MSI2 expression vector (pF5A-MSI2), respectively. Knockdown of MSI2 by siR-MSI2 induced cell growth inhibition along with

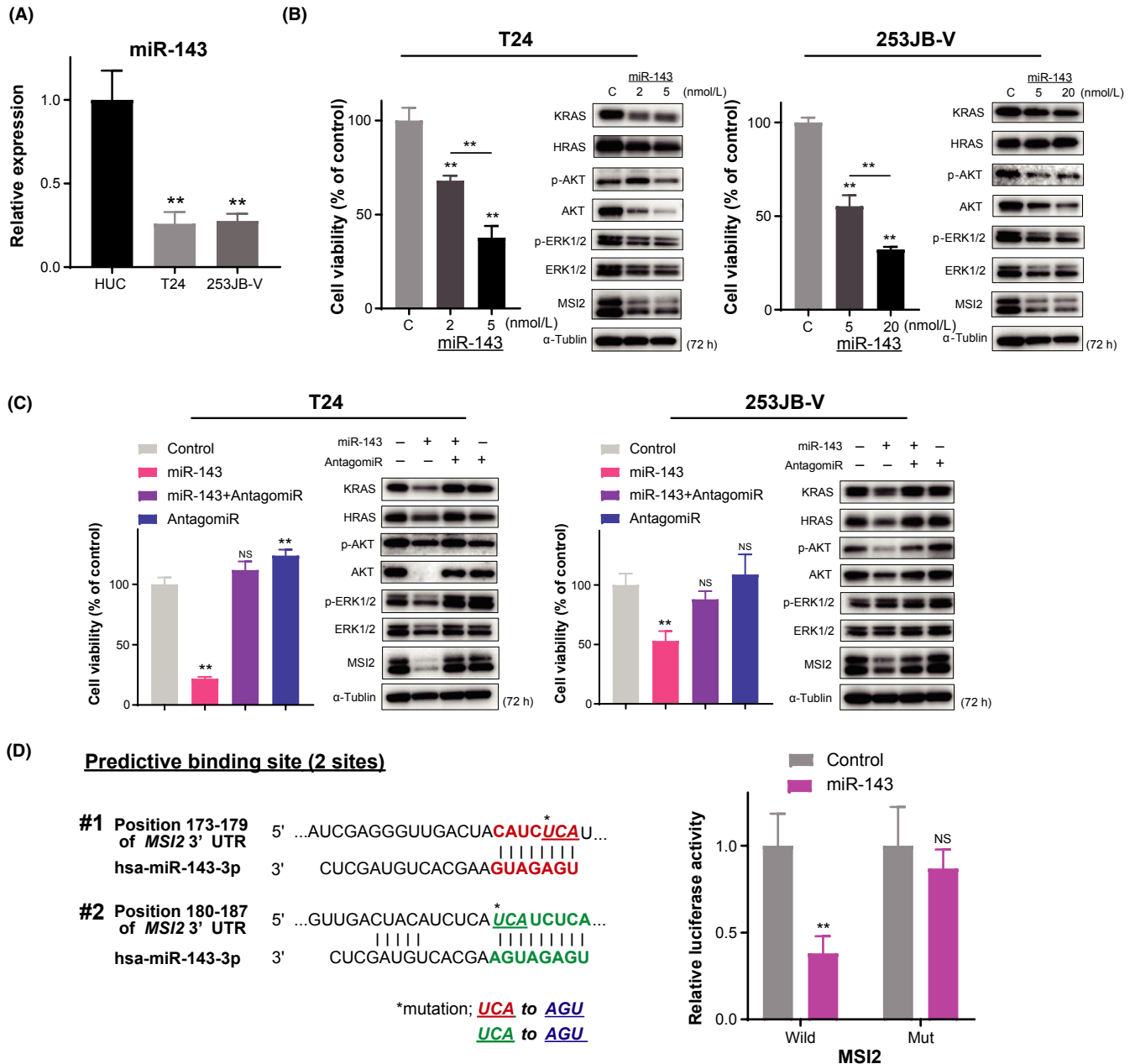


FIGURE 2 Ectopic expression of microRNA (miR)-143 induces significant downregulation of KRAS and Musashi-2 (MSI2) through RNA interference. A, Relative expression levels of miR-143 in T24 and 253JB-V cells. B, Dose-dependent effect of miR-143 on cell viability and protein expression levels of the target genes. C, Above effects of miR-143 were verified in cells treated with antagomiR-143. D, Luciferase activities after cotransfection with control or miR-143 and wild-type or mutant-type pMIR vectors having the predictive miR-143 binding site in the 3'UTR of *MSI2*. Left panel shows complementation in the regions of the 3'UTR of *MSI2* mRNA (positions 173-179: #1 and 180-187: #2) to the mature miR-143. Colored (red and green) sequences of two sites indicate the predicted binding sites for miR-143. The nucleotide sequence of the mutated site is shown in blue. ** $P < .01$. Means + SD indicated by error bars are shown. NS, not significant

downregulation of KRAS (Figure 4A). In contrast, overexpression of *MSI2* promoted cell proliferation and upregulated KRAS (Figure 4B). Importantly, no significant change in *KRAS* mRNA levels was observed in the case of either silencing or overexpression of *MSI2* (Figure 4A,B). On the contrary, expression levels of *HRAS* mRNA corresponded to those of *MSI2*. Taken together, these data suggested that *KRAS* and *HRAS* were downstream of *MSI2* and that *MSI2* may have post-transcriptionally regulated the transcripts of *KRAS* and

HRAS. Notably, the expression of *MSI2* was also affected by *KRAS* or *HRAS*, because either knockdown of *KRAS* or *HRAS* caused a decrease in the expression of *MSI2* protein (Figure 4C). Also, silencing of either *KRAS* or *HRAS* caused the expression of *HRAS* or *KRAS*, respectively, to decrease. These results indicated that *MSI2* and *KRAS* or *HRAS* are coordinated with each other, although it is difficult to clarify how *MSI2* interacts with *KRAS* and *HRAS*, given the complicated nature of RAS signaling networks.

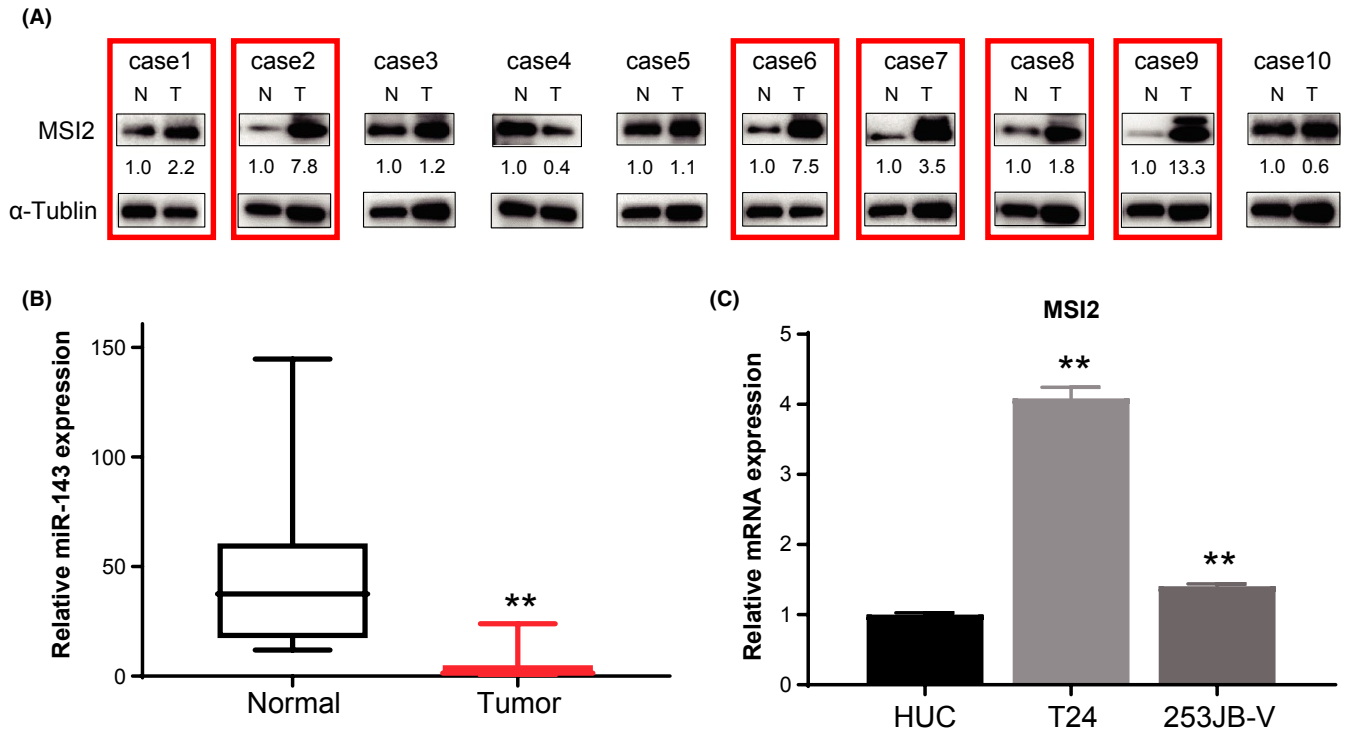


FIGURE 3 Expression of Musashi-2 (MSI2) in clinical bladder cancer (BC) samples and cell lines. A, Protein expression levels of MSI2 in 10 BC tumor tissue samples from BC patients. Overexpression of MSI2 in tumor samples is highlighted by red-colored boxes. N, normal; T, tumor in the same patient. B, Relative expression levels of MSI2 in T24 and 253JB-V cells. C, Relative mRNA expression level of MSI2 in BC cell lines compared with that in HUC. ** $P < .01$. Means + SD indicated by error bars are shown. HUC, human urothelial cell; miR, microRNA

3.5 | Musashi-2 directly binds to mRNA of KRAS

To clarify whether or not MSI2 bound directly to mRNAs of *KRAS* and *HRAS*, using BC cells, we first carried out MSI2-immunoprecipitation (IP) followed by qRT-PCR. Western blot analysis, carried out as a quality check, showed that MSI2 was detected in input and MSI2-IP samples only, not in the control IgG-IP sample. qRT-PCR findings showed that the MSI2-immunoprecipitated RNA fraction was significantly enriched in *KRAS* mRNA (Figure 5A), whereas there was no enrichment of *HRAS* mRNA in IgG or MSI2 fractions. These data suggested that MSI2 directly bound to *KRAS* but not to *HRAS*. Therefore, the data on *HRAS* observed in Figure 4A,B were supposedly as a result of an indirect impact of MSI2.

In addition, to determine the direct interaction between MSI2 and *KRAS* mRNA, we cloned the predicted MSI2 binding site UAGUA in the 3'UTR region of *KRAS* mRNA in a reporter plasmid vector (Figure 5B). Results of the luciferase reporter assay indicated that activity of wild-type pMIR-*KRAS* was decreased by siR-MSI2 compared with that obtained with control siRNA, indicating that the activity paralleled the level of MSI2 protein expression. On the contrary, decrease in the activity of the pMIR vector was almost canceled when the mutated MSI2 binding site AUCAU was used. Thus, these data clearly showed the promoting roles of MSI2 in the translation step of luciferase mRNAs.

To examine direct interaction between MSI2 and UAGUA, we next used the SPR assay. To this end, a recombinant MSI2 protein containing the two RNA-binding domains was expressed (Figure S5) and immobilized on a sensor-chip surface. A synthetic 15-mer *KRAS* mRNA containing UAGUA or its scrambled sequence as a control was injected over the sensor chip. As shown in the left panel of Figure 5C, the UAGUA sequence gave the highest binding response to the immobilized MSI2 (reaching 50 resonance units at 10 μ mol/L). In addition, a dissociation constant (K_d) of UAGUA for MSI2 was 2-5-fold lower than that for the control RNA (right panel of Figure 5C), suggesting that MSI2 preferentially bound to the UAGUA sequence.

Collectively, these data showed that MSI2 directly interacted with *KRAS* mRNA by recognizing and binding to one of the specific UAGUA sequences.

3.6 | Musashi-2 post-transcriptionally enhances translation of KRAS

To investigate how MSI2 regulates the processing of *KRAS* mRNAs after transcription, we first examined the localization of MSI2 in cells by using immunofluorescence. MSI2 was located mainly in the cytoplasm in T24 and 253JB-V cells (Figure 6A) in agreement with the reports in a public database (The Human Protein Atlas).

Cellular localization of MSI2 and the findings in the current study suggest that MSI2 might have the ability to regulate the

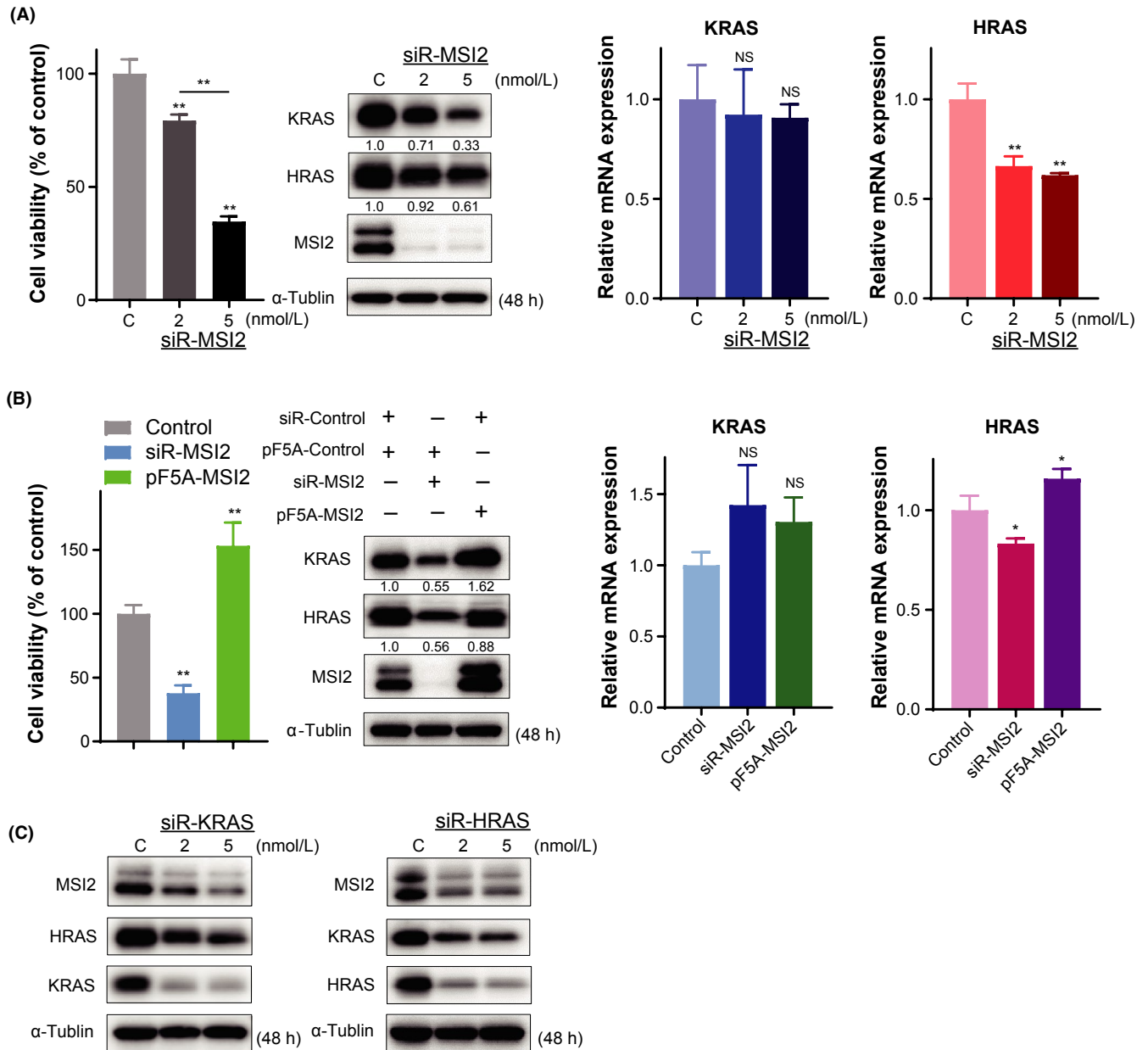


FIGURE 4 Relationship between Musashi-2 (MSI2) and KRAS or HRAS in expression profiles of T24 cells. A, Effects of MSI2 knockdown using siRNA on cell growth (left panel). Protein and mRNA expression levels of KRAS and HRAS after siR-MSI2 transfection (middle and right panels). B, Effects of MSI2 knockdown and overexpression on cell growth (left panel). Protein and mRNA expression levels of KRAS and HRAS in MSI2-silenced and -overexpressed cells (middle and right panels). C, MSI2 and RAS protein profiles after transfection with siR-KRAS or siR-HRAS. * $P < .05$; ** $P < 0.01$. Means + SD indicated by error bars are shown. NS, not significant

stability or translation of target mRNAs.³³ To determine whether MSI2 could regulate the stability of KRAS mRNA, we estimated the rate of mRNA decay after treatment with DRB. Time-course RNA decay curves for KRAS mRNA were prepared from qRT-PCR data after DRB treatment of cells transfected with pF5A-control or pF5A-MSI2. As a result, the half-life of KRAS mRNA was not significantly changed in either case, whereas overexpression of MSI2 was achieved in the case of pF5A-MSI2 transfection (Figure 6B). These data thus showed that MSI2 functioned to enhance the translation of KRAS mRNA rather than to stabilize the mRNA, the finding of which is well supported by the results given in Figure 4A,B. To

further validate that MSI2 regulated the translation, we assessed the expression of translational initiator eIF4E by western blot analysis. Notably, knockdown of MSI2 induced the downregulation of eIF4E (Figure 6C). These data suggested that MSI2 played a role in enhancing translation. Furthermore, western blot analysis showed that MSI2 and KRAS were co-upregulated in six cases of 10 clinical BC samples compared with their expression in normal bladder tissues (Figure 6D). In Lee's cohort,³⁴ there was a significant positive correlation of mRNA expression levels between MSI2 and KRAS in human BC (Figure 6E). These data suggested that the patients, which had abundant MSI2 mRNA, could have increment of KRAS protein

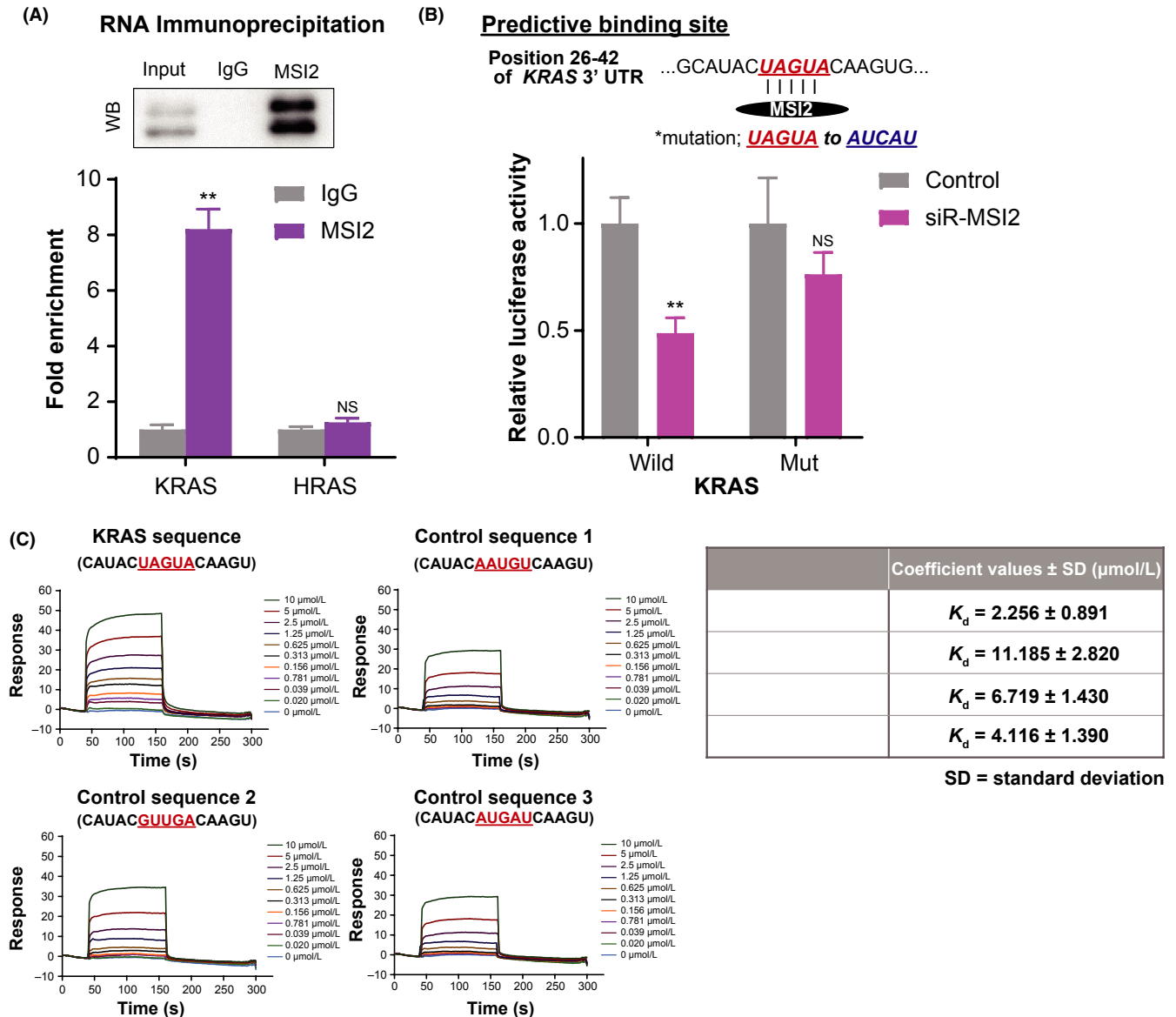


FIGURE 5 Musashi-2 (MSI2) directly binds to UAGUA in 3'UTR of KRAS mRNA. A, RNA-immunoprecipitation of MSI2 complexes with anti-MSI2 or control anti-rabbit IgG antibody, followed by qRT-PCR of KRAS and HRAS. Relative enrichment was calculated by enrichment over the control. Western blot analysis as a quality check of immunoprecipitated MSI2 is also shown. B, Luciferase activities after cotransfection with control or siR-MSI2 and wild-type or mutant-type pMIR vectors having the predictive MSI2 binding site in the 3'UTR of KRAS. Upper panel shows the position 26-42 of the 3'UTR of KRAS mRNA. Colored sequences indicate the predicted binding site for MSI2. Site of the mutated sequence is shown in blue. ** $P < 0.01$. Means + SD indicated by error bars are shown. NS, not significant. C, Representative surface plasmon resonance (SPR) sensorgrams for binding of MSI2 to synthetic RNAs containing KRAS mRNA (UAGUA) or its scrambled sequences (AAUGU, GUUGA, and AUGAU) (left panel). Dissociation constants between MSI2 protein and RNAs shown in the left panel. Average ± SD from three experiments (right panel)

expression through efficient translation by MSI2. Furthermore, we showed that the silencing effect of KRAS by ectopic expression with syn-miR-143 was certainly canceled by overexpression of MSI2 (Figure S6). This finding suggested that downregulated expression of MSI2 by miR-143 was significant in the growth of BC cells.

Collectively, these data indicated that MSI2 functioned to accelerate the translation of KRAS mRNA in the cytoplasm and had crucial roles as a KRAS enhancer in BC cells. This machinery was closely correlated with KRAS networks, in which there was a positive circuit

for enhancement of KRAS mRNA expression by KRAS effector signaling (AKT and ERK)¹⁰ (Figures 7, S7 and S8).

3.7 | MicroRNA-143/MSI2/KRAS cascade on T24 cell-xenografted tumors in nude mice

We have clarified the novel miR-143/MSI2/KRAS cascade in vitro. To further validate the cascade between miR-143, MSI2 and KRAS, we examined the antitumor effect by using syn-miR-143 and siR-MSI2

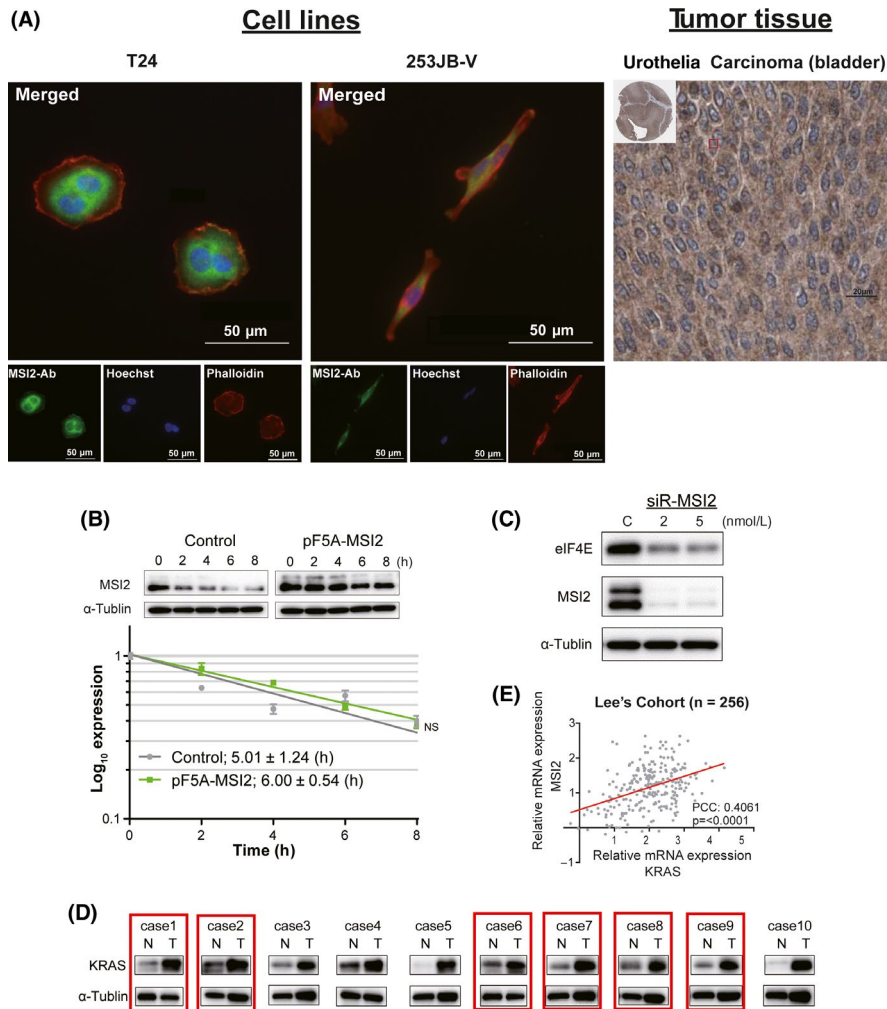


FIGURE 6 Cell localization of Musashi-2 (MSI2) and functions against *KRAS* mRNA. A, Immunofluorescence of MSI2 (green), a nucleic marker, Hoechst 33342 (blue), and an actin marker, Phalloidin (red) in T24 and 253JB-V cells (left panel). Immunohistochemistry images as obtained from the Human Protein Atlas also show MSI2 in bladder carcinoma (BC) tissue (right panel). B, *KRAS* mRNA stability curves were plotted as qRT-PCR expression with time. ANCOVA was used for determining statistical significance. Mean standard error is indicated for each time point. Half-life in hours was calculated from the stability curves. NS, not significant. C, Protein expression of translational initiator eIF4E in MSI2-silenced cells. D, Protein expression levels of MSI2 and *KRAS* in 10 tumor tissue samples from BC patients. Cases with co-upregulated MSI2 and *KRAS* in the tumor samples are highlighted by red boxes. The samples are the same as in Figure 3A. N, normal; T, tumor in the same patient. E, Correlation of mRNA expression levels between *MSI2* and *KRAS* in human BC samples from Lee's cohort (n = 256) estimated by bioinformatics. PCC, Pearson's correlation coefficient

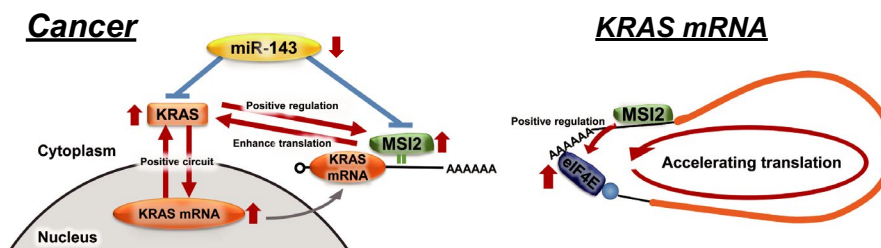


FIGURE 7 Schematic diagrams showing the roles of Musashi-2 (MSI2) in *KRAS* networks and the association of MSI2 with *KRAS* mRNA. MicroRNA (miR)-143/MSI2/*KRAS* cascade (left panel) and possible machinery for MSI2-mediated enhancement of the translation of *KRAS* mRNA (right panel)

in vivo. As shown in Figure 8A, growth suppression of tumors was observed in the groups treated with siR-MSI2 or syn-miR-143. In addition, the tumor-suppressive effect of syn-miR-143 was greater

than that of siR-MSI2. Western blot analysis of the tissue samples from grafted tumors showed that MSI2 was significantly silenced in both treated groups. Furthermore, decreased expression of *KRAS*

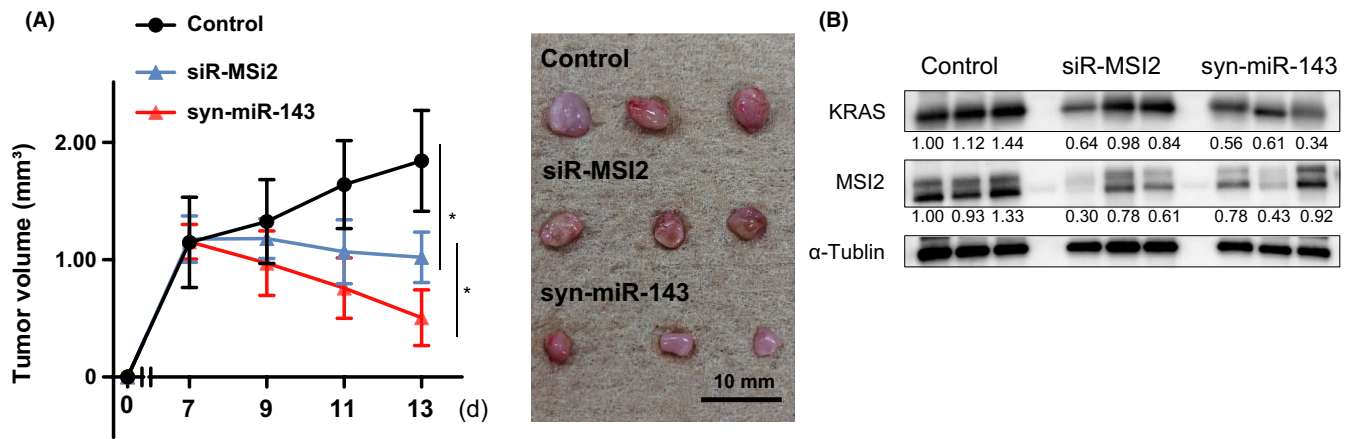


FIGURE 8 Antitumor activity of siR-MSI2 and syn-miR-143 in T24 cell-xenografted mice. A, Changes in tumor size of mice treated with control siRNA, siR-MSI2 or syn-miR-143 ($n = 3$; left panel). (Right panel) Representative photograph of tumors. Upper, middle and lower photos show the tumors from control and treated mice, respectively. B, Protein expression levels of MSI2 and KRAS in control, siR-MSI2 or syn-miR-143-treated tumor tissues. * $P < .05$. Means \pm SD indicated by error bars are shown. miR, microRNA; MSI2, Musashi-2

protein was also shown in both groups as it had been found in vitro (Figures 2B and 4A), and the KRAS-silencing effect of syn-miR-143 was greater than that of siR-MSI2 (Figure 8B). These findings suggested that MSI2 contributed to the growth of the engrafted tumor through upregulation of KRAS, and that the miR-143/MSI2/KRAS cascade could exist even in an in vivo experiment.

4 | DISCUSSION

In the current study, we clarified a novel network operating miR-143, MSI2 and KRAS (Figure 7). We were also able to show that the expression of KRAS was affected by MSI2 through binding of the latter to KRAS mRNA, the finding of which was validated by RNA-IP, SPR, and the expression profiles of the genes involved. Previously, we showed that miR-143 directly silences KRAS signaling networks;^{10,17} and Dong et al³⁰ reported that miR-143 also targets RNA-binding protein MSI2. However, the association between these targets of miR-143, KRAS and MSI2 had not been previously reported. Given the earlier reports that MSI2 has been suggested to interact preferentially with the UAG-containing motifs in the 3'UTR region of its target RNAs,^{21,35-37} we predicted the binding site in KRAS mRNA to be UAGUA and showed by a using luciferase reporter assay and the SPR technique (Figure 5B,C) that MSI2 protein preferentially binds to the sequence. In addition, it was earlier reported that MSI2 has functions to affect the stabilization or translation of its target mRNAs.^{21,30,38} Based on our results, MSI2 did not impact the stability of KRAS mRNA despite its direct binding to it (Figure 6B). Given that MSI2 positively regulated the translational initiator eIF4E (Figure 6C), we propose that MSI2 functioned to enhance the translation of KRAS mRNA rather than its stabilization. With regard to the role of translational regulation, MSI2 is regulated by site-specific phosphorylation, which converts MSI2 from a repressor to an activator of target mRNA translation, and MAPK and Ringo/CDK contribute

to MSI2 regulatory phosphorylation, as does MSI1.^{39,40} MAPK also contributes to the translational machinery including eIF4E.⁴¹ MSI2 may be included in the cascades, and MAPK positively regulates eIF4E through phosphorylation of MSI2. In addition, given the RAS signaling pathways, KRAS and HRAS could regulate MSI2 through MAPK indirectly. Indeed, it is reasonable that MSI2 was downregulated in cells by knockdown of KRAS and HRAS, in which ERK1/2 was also inhibited (Figures 1B and 4C).

We demonstrated an association between the specific sequence UAGUA and the ability of MSI2 to enhance the translation of its target mRNA. However, the SPR technique showed that the control sequences, despite the absence of a UAG motif, gave a weak binding response to MSI2 protein (Figure 5C). These data suggested that the specificity of MSI2 binding to transcripts may not be so high. The impact of MSI2 on its target RNAs could be due not only to binding ability, but also to other mechanisms. The two RNA recognition motif (RRM) of MSI2 are possibly involved in the mechanism. Biochemical and structural studies have suggested that RRM1 contributes the majority of the binding energy and specificity, whereas RRM2 has a more supportive role.³⁷ In addition, Bennett et al²¹ reported that these two RRM may provide a mechanism for MSI2 to distinguish its veritable targets. However, this machinery is presently barely understood and further validation is warranted.

In the present study, we clarified that MSI2 directly targeted KRAS, promoting translation of its mRNA. The RTK/RAS pathway has been reported to be involved in the regulation of cell proliferation in several cancers.⁴²⁻⁴⁵ Recent precision medicine studies showed that gene alterations in RTK/RAS pathways occurred in up to 60% of BC patients.⁴⁶ Among these signaling pathways, in particular, up to 80% of non-muscle invasive BC (NMIBC) harbor activating point mutations in FGFR3,^{47,48} which activate the RAS/MAPK pathway.^{4,5,49} Moreover, the alteration of KRAS occurs more frequently than that of HRAS.^{2,3} Thus, KRAS and KRAS signaling networks are dominant pathways in BC. Previously, we have clarified the signaling networks. The "positive circuit" through the constitutive KRAS activation-stimulation of effector signaling pathways (PI3K/AKT and MAPK) occurs in colorectal cancer, resulting in enhanced

nuclear KRAS transcription.¹⁰ As shown in Figure S7, this cascade was also seen in BC cell lines and, again, the “positive circuit” also occurred in HRAS signaling networks. These data suggested that KRAS and HRAS interacted with each other, indicating that either MSI2 or miR-143 indirectly affected the expression of HRAS by regulating KRAS. Indeed, inhibition of the signals of ERK and AKT occurred, resulting in indirect regulation of HRAS expression in the case of treatment with siR-MSI2 or syn-miR-143 (Figures 2B and S8).

Recently, it was reported that miR-143 has a significant antitumor role in BC. Lin et al¹⁵ reported that transfection of BC cells with miR-143 significantly inhibited cell proliferation through decreased expression of RAS protein. Wang et al⁵⁰ showed that overexpression of miR-143 inhibited cell proliferation in BC. Furthermore, we demonstrated previously that syn-miR-143 functions as a tumor suppressor in BC cells.^{17,32} In an earlier study, we also showed that miR-143 directly targets KRAS signaling networks.¹⁰ Furthermore, it was reported that miR-143 also directly targets MSI2 in cervical cancer.³⁰ In the present study, we clarified the novel association between MSI2 and KRAS, both of which are targets of miR-143, validating the interaction between MSI2 and the UAGUA sequence of the KRAS transcript in vitro (Figures 4 and 5, S6). Previously, genome-wide analyses demonstrated that MSI2 binds to a multitude of target genes.³⁷ Fox et al⁵¹ validated targets C-MET, BRD4, and HMGA2 in pancreatic cancer, and Park et al⁵² validated 48 genes in hematopoietic stem cells and 11 genes in leukemia stem cells.³⁸ Thus, as MSI2 binds to a great number of targets, KRAS cannot be listed at the top in genome-wide analysis of MSI2-ribonucleoproteins. Syn-miR-143 has allowed us to propose the possibility of association between the two proteins, resulting in a better understanding of the novel miR-143/MSI2/KRAS expression system (Figure 7).

Collectively, we showed that miR-143 directly impacted MSI2 expression through its RNAi action, which also effectively inhibited KRAS networks as a novel mechanism in human BC. Moreover, this evidence was confirmed by the results of an in vivo experiment (Figure 8). Taken together, these findings indicated the complicated nature of KRAS networks and the tight control of their maintenance.

ACKNOWLEDGMENTS

This work was carried out with the support of SHIONOGI. This work was supported by the Project for Cancer Research and Therapeutic Evolution (P-CREATE) from Japan Agency for Medical Research and Development (AMED) (16cm0106202 h0001 to YA).

DISCLOSURE

Authors declare no conflicts of interest for this article.

ORCID

Takuya Tsujino  <https://orcid.org/0000-0003-1559-1889>

Kohei Taniguchi  <https://orcid.org/0000-0003-0648-1370>

Kazumasa Komura  <https://orcid.org/0000-0003-4157-1929>

Haruka Shinohara  <https://orcid.org/0000-0001-8326-1203>

REFERENCES

- Siegel RL, Miller KD, Jemal A. Cancer statistics, 2017. *CA Cancer J Clin.* 2017;67:7-30.
- Robertson AG, Kim J, Al-Ahmadie H, et al. Comprehensive molecular characterization of muscle-invasive bladder cancer. *Cell.* 2017;171:540-556. e25.
- Springer SU, Chen CH, Rodriguez Pena MDC, et al. Non-invasive detection of urothelial cancer through the analysis of driver gene mutations and aneuploidy. *Elife.* 2018;7:e32143.
- Oliveras-Ferraros C, Cufi S, Queralt B, et al. Cross-suppression of EGFR ligands amphiregulin and epiregulin and de-repression of FGFR3 signalling contribute to cetuximab resistance in wild-type KRAS tumour cells. *Br J Cancer.* 2012;106:1406-1414.
- Touat M, Ileana E, Postel-Vinay S, Andre F, Soria JC. Targeting FGFR signaling in cancer. *Clin Cancer Res.* 2015;21:2684-2694.
- Tsai FD, Lopes MS, Zhou M, et al. K-Ras4A splice variant is widely expressed in cancer and uses a hybrid membrane-targeting motif. *Proc Natl Acad Sci USA.* 2015;112:779-784.
- Jinesh GG, Sambandam V, Vijayaraghavan S, Balaji K, Mukherjee S. Molecular genetics and cellular events of K-Ras-driven tumorigenesis. *Oncogene.* 2018;37:839-846.
- Chen X, Guo X, Zhang H, et al. Role of miR-143 targeting KRAS in colorectal tumorigenesis. *Oncogene.* 2009;28:1385-1392.
- Akao Y, Nakagawa Y, Iio A, Naoe T. Role of microRNA-143 in Fas-mediated apoptosis in human T-cell leukemia Jurkat cells. *Leuk Res.* 2009;33:1530-1538.
- Akao Y, Kumazaki M, Shinohara H, et al. Impairment of K-Ras signaling networks and increased efficacy of epidermal growth factor receptor inhibitors by a novel synthetic miR-143. *Cancer Sci.* 2018;109:1455-1467.
- Akao Y, Nakagawa Y, Naoe T. MicroRNAs 143 and 145 are possible common onco-microRNAs in human cancers. *Oncol Rep.* 2006;16:845-850.
- Akao Y, Nakagawa Y, Kitade Y, Kinoshita T, Naoe T. Downregulation of microRNAs-143 and -145 in B-cell malignancies. *Cancer Sci.* 2007;98:1914-1920.
- Akao Y, Nakagawa Y, Hirata I, et al. Role of anti-oncomirs miR-143 and -145 in human colorectal tumors. *Cancer Gene Ther.* 2010;17:398-408.
- Takagi T, Iio A, Nakagawa Y, Naoe T, Tanigawa N, Akao Y. Decreased expression of microRNA-143 and -145 in human gastric cancers. *Oncology.* 2009;77:12-21.
- Lin T, Dong W, Huang J, et al. MicroRNA-143 as a tumor suppressor for bladder cancer. *J Urol.* 2009;181:1372-1380.
- Zhou H, Tang K, Xiao H, et al. A panel of eight-miRNA signature as a potential biomarker for predicting survival in bladder cancer. *J Exp Clin Cancer Res.* 2015;34:53
- Noguchi S, Yasui Y, Iwasaki J, et al. Replacement treatment with microRNA-143 and -145 induces synergistic inhibition of the growth of human bladder cancer cells by regulating PI3K/Akt and MAPK signaling pathways. *Cancer Lett.* 2013;328:353-361.
- Sakakibara S, Nakamura Y, Satoh H, Okano H. Rna-binding protein Musashi2: developmentally regulated expression in neural precursor cells and subpopulations of neurons in mammalian CNS. *J Neurosci.* 2001;21:8091-8107.
- Wang S, Li N, Yousefi M, et al. Transformation of the intestinal epithelium by the MSI2 RNA-binding protein. *Nat Commun.* 2015;6:6517.
- Zearfoss NR, Deveau LM, Clingman CC, et al. A conserved three-nucleotide core motif defines Musashi RNA binding specificity. *J Biol Chem.* 2014;289:35530-35541.
- Bennett CG, Riemondy K, Chapnick DA, et al. Genome-wide analysis of Musashi-2 targets reveals novel functions in governing epithelial cell migration. *Nucleic Acids Res.* 2016;44:3788-3800.

22. Kanemura Y, Mori K, Sakakibara S, et al. Musashi1, an evolutionarily conserved neural RNA-binding protein, is a versatile marker of human glioma cells in determining their cellular origin, malignancy, and proliferative activity. *Differentiation*. 2001;68:141-152.
23. Hemmati HD, Nakano I, Lazareff JA, et al. Cancerous stem cells can arise from pediatric brain tumors. *Proc Natl Acad Sci USA*. 2003;100:15178-15183.
24. Shu HJ, Saito T, Watanabe H, et al. Expression of the Musashi1 gene encoding the RNA-binding protein in human hepatoma cell lines. *Biochem Biophys Res Comm*. 2002;293:150-154.
25. Barbouti A, Hoglund M, Johansson B, et al. A novel gene, MSI2, encoding a putative RNA-binding protein is recurrently rearranged at disease progression of chronic myeloid leukemia and forms a fusion gene with HOXA9 as a result of the cryptic t(7;17)(p15;q23). *Can Res*. 2003;63:1202-1206.
26. Kharas MG, Lengner CJ, Al-Shahrou F, et al. Musashi-2 regulates normal hematopoiesis and promotes aggressive myeloid leukemia. *Nat Med*. 2010;16:903-908.
27. Kudinov AE, Deneka A, Nikonova AS, et al. Musashi-2 (MSI2) supports TGF-beta signaling and inhibits claudins to promote non-small cell lung cancer (NSCLC) metastasis. *Proc Natl Acad Sci USA*. 2016;113:6955-6960.
28. Guo K, Cui J, Quan M, et al. The novel KLF4/MSI2 signaling pathway regulates growth and metastasis of pancreatic cancer. *Clin Cancer Res*. 2017;23:687-696.
29. Yang C, Zhang W, Wang L, et al. Musashi-2 promotes migration and invasion in bladder cancer via activation of the JAK2/STAT3 pathway. *Lab Invest*. 2016;96:950-958.
30. Dong P, Xiong Y, Hanley SJB, Yue J, Watari H. Musashi-2, a novel oncoprotein promoting cervical cancer cell growth and invasion, is negatively regulated by p53-induced miR-143 and miR-107 activation. *J Exp Clin Cancer Res*. 2017;36:150.
31. Chen CY, Ezzeddine N, Shyu AB. Messenger RNA half-life measurements in mammalian cells. *Methods Enzymol*. 2008;448:335-357.
32. Noguchi S, Mori T, Hoshino Y, et al. MicroRNA-143 functions as a tumor suppressor in human bladder cancer T24 cells. *Cancer Lett*. 2011;307:211-220.
33. Gerstberger S, Hafner M, Tuschl T. A census of human RNA-binding proteins. *Nat Rev Genet*. 2014;15:829-845.
34. Lee J-S, Leem S-H, Lee S-Y, et al. Expression signature of E2F1 and its associated genes predict superficial to invasive progression of bladder tumors. *J Clin Oncol*. 2010;28:2660-2667.
35. Katz Y, Li F, Lambert NJ, et al. Musashi proteins are post-transcriptional regulators of the epithelial-luminal cell state. *eLife*. 2014;3:e03915.
36. Lan L, Xing M, Douglas JT, Gao P, Hanzlik RP, Xu L. Human oncoprotein Musashi-2 N-terminal RNA recognition motif backbone assignment and identification of RNA-binding pocket. *Oncotarget*. 2017;8:106587-106597.
37. Kudinov AE, Karanicolas J, Golemis EA, Boumber Y. Musashi RNA-binding proteins as cancer drivers and novel therapeutic targets. *Clin Cancer Res*. 2017;23:2143-2153.
38. Park SM, Gonen M, Vu L, et al. Musashi2 sustains the mixed-lineage leukemia-driven stem cell regulatory program. *J Clin Invest*. 2015;125:1286-1298.
39. Arumugam K, MacNicol MC, Wang Y, et al. Ringo/cyclin-dependent kinase and mitogen-activated protein kinase signaling pathways regulate the activity of the cell fate determinant Musashi to promote cell cycle re-entry in *Xenopus* oocytes. *J Biol Chem*. 2012;287:10639-10649.
40. MacNicol MC, Cragle CE, McDaniel FK, et al. Evasion of regulatory phosphorylation by an alternatively spliced isoform of Musashi2. *Sci Rep*. 2017;7:11503.
41. Roux PP, Topisirovic I. Signaling pathways involved in the regulation of mRNA translation. *Mol Cell Biol*. 2018;38:e00070-18.
42. Eser S, Schnieke A, Schneider G, Saur D. Oncogenic KRAS signalling in pancreatic cancer. *Br J Cancer*. 2014;111:817-822.
43. Lemieux E, Cagnol S, Beaudry K, Carrier J, Rivard N. Oncogenic KRAS signalling promotes the Wnt/beta-catenin pathway through LRP6 in colorectal cancer. *Oncogene*. 2015;34:4914-4927.
44. Wong GS, Zhou J, Liu JB, et al. Targeting wild-type KRAS-amplified gastroesophageal cancer through combined MEK and SHP2 inhibition. *Nat Med*. 2018;24:968-977.
45. Regad T, Targeting RTK. Signaling pathways in cancer. *Cancers*. 2015;7:1758-1784.
46. Sanchez-Vega F, Mina M, Armenia J, et al. Oncogenic signaling pathways in the cancer genome Atlas. *Cell*. 2018;173:321-337. e10.
47. Knowles MA, Hurst CD. Molecular biology of bladder cancer: new insights into pathogenesis and clinical diversity. *Nat Rev Cancer*. 2015;15:25-41.
48. Inamura K. Bladder cancer: new insights into its molecular pathology. *Cancers*. 2018;10:100.
49. Yadav V, Zhang X, Liu J, et al. Reactivation of mitogen-activated protein kinase (MAPK) pathway by FGF receptor 3 (FGFR3)/Ras mediates resistance to vemurafenib in human B-RAF V600E mutant melanoma. *J Biol Chem*. 2012;287:28087-28098.
50. Wang H, Li Q, Niu X, et al. miR-143 inhibits bladder cancer cell proliferation and enhances their sensitivity to gemcitabine by repressing IGF-1R signaling. *Oncol Lett*. 2017;13:435-440.
51. Fox RG, Lytle NK, Jaquish DV, et al. Image-based detection and targeting of therapy resistance in pancreatic adenocarcinoma. *Nature*. 2016;534:407-411.
52. Park SM, Deering RP, Lu Y, et al. Musashi-2 controls cell fate, lineage bias, and TGF-beta signaling in HSCs. *J Exp Med*. 2014;211:71-87.

SUPPORTING INFORMATION

Additional supporting information may be found online in the Supporting Information section at the end of the article.

How to cite this article: Tsujino T, Sugito N, Taniguchi K, et al. MicroRNA-143/Musashi-2/KRAS cascade contributes positively to carcinogenesis in human bladder cancer. *Cancer Sci*. 2019;110:2189-2199. <https://doi.org/10.1111/cas.14035>